MAZUR MANIFOLDS AND CORKS WITH SMALL SHADOW COMPLEXITIES

HIRONOBU NAOE

Abstract. In this paper we show that there exist infinitely many Mazur type manifolds and corks with shadow complexity one among the 4-manifolds constructed from contractible special polyhedra having one true vertex by using the notion of Turaev's shadow. We also find such manifolds among 4-manifolds constructed from Bing's house. Our manifolds with shadow complexity one contain the Mazur manifolds $W^{\pm}(l,k)$ which were studied by Akbulut and Kirby.

1. Introduction

The study of *corks* is crucial to understand smooth structures on 4-manifolds due to the following theorem: *For every exotic (i.e. homeomorphic but non-diffeomorphic) pair of simply connected closed 4-manifolds, one is obtained from the other by removing a contractible submanifold of codimension* 0 *and gluing it via an involution on the boundary. Furthermore, the contractible submanifold and its complement can always be compact Stein 4-manifolds.* The contractible 4-manifold has since been called a *cork*. This theorem was first proved independently by Matveyev [22] and Curtis, Freedman, Hsiang and Stong [15], and strengthened by Akbulut and Matveyev [5] afterward. The first cork was found by Akbulut in [1] among *Mazur manifolds*. Here a *Mazur manifold* is a contractible 4-manifold which is not bounded by the 3-sphere and has a handle decomposition consisting of a single 0-handle, a single 1-handle and a single 2-handle. Akbulut and Yasui generalized the example in [1] and constructed many exotic pairs of 4-manifolds by using the corks $W_n, \overline{W}_n$ in [6, 7].

On the other hand, Turaev introduced the notion of a *shadow* for the purpose of study of quantum invariants of 3- and 4-manifolds in 1990s. A shadow is an almost-special polyhedron P which is locally flat and properly embedded in a compact oriented 4-manifold W with boundary and a strongly deformation retract of W. By the study of Turaev, W is uniquely recovered from the shadow P with a coloring assigned to each region of P. This operation is called Turaev's reconstruction. The coloring is a half-integer, called a *gleam*. By this reconstruction, a shadow with gleam provides a differential structure of W uniquely. We refer the reader to [12, 13], in

2010 *Mathematics Subject Classification.* Primary 57R65; Secondary 57M20, 57R55.
Key words and phrases. 4-manifold, shadow, exotic, Akbulut's cork.

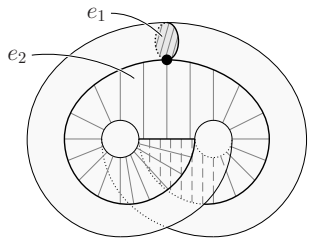

Figure 1. The abalone has only one true vertex and two regions. Let e_1 be the disk region in the upper part of the figure, and let e_2 be the other region. We can check that e_2 is a disk easily.

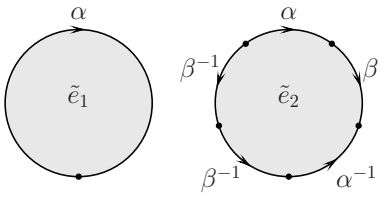

Figure 2. This polyhedron has only one true vertex and two disk regions. This can not be embedded in $\mathbb{R}^3$.

which Costantino studied Stein structures, Spin^c structures and complex structures on 4-manifolds by using shadows.

In this paper, we focus on the *shadow complexity* to align all corks according to their complexities. The shadow complexity of a 4-manifold W is defined by the minimal number of true vertices among all shadows of W, which was introduced by Costantino in [11]. See Definition 3.5 for details. A classification of closed 4-manifolds with shadow complexity zero had been studied by Costantino in [11] and Martelli in [21]. As a subsequent project, we study 4-manifolds constructed from contractible special shadows with complexity 1 or 2 and find infinitely many Mazur type manifolds and corks. As a related topic, Costantino asked in [11] what pair of exotic 4-manifolds has the minimal special shadow complexity and pointed out that the complexity is at most 3.

We first focus on the shadows with one vertex. In [17, 18], Ikeda classified acyclic special polyhedra with one true vertex and showed that there exist just two such polyhedra. One is called the abalone, shown in Figure 1, and the other is a polyhedron shown in Figure 2. We denote by A the abalone, and by $\tilde{A}$ the other one. They are contractible since they are acyclic and simply connected. To find corks with special shadow complexity 1, we have only to study A and $\tilde{A}$, by the above classification. Let $A(m,n)$ be the compact oriented 4-manifold obtained by Turaev's reconstruction from A with gleams $\mathrm{gl}(e_1) = m, \mathrm{gl}(e_2) = n$ (see Figure 1), and let $\tilde{A}(m, n-\frac{1}{2})$ be the one constructed from $\tilde{A}$ with gleams $\mathrm{gl}(\tilde{e}_1) = m, \mathrm{gl}(\tilde{e}_2) = n - \frac{1}{2}$ (see Figure 2). Note that the above n and m are integers. The main results of this paper in the case of complexity 1 are the following.

Theorem 1.1. *If $m \neq 0$, $A(m,n)$ is Mazur type. Moreover, $A(m,n)$ and $A(m',n')$ are not homeomorphic unless $m = m'$.*

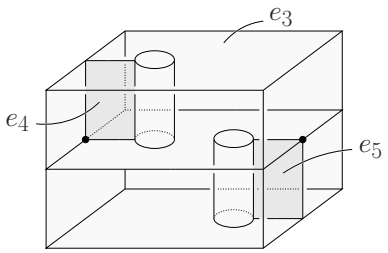

Figure 3. Bing's house has two true vertices and three disk regions. Let e_4 and e_5 be the disk regions which are partitions put first and second floor respectively, and let e_3 be the last region. We can check that e_3 is a disk easily.

Theorem 1.2.

(1) *If $m \neq 0$, $\tilde{A}(m, n-\frac{1}{2})$ is Mazur type. Moreover, $\tilde{A}(m, n-\frac{1}{2})$ and $\tilde{A}(m', n'-\frac{1}{2})$ are not homeomorphic unless $m = m'$.*
(2) *The pair $(\tilde{A}(m, -\frac{3}{2}), \tilde{f}_m)$ is a cork if $m < 0$.*

Here $\tilde{f}_m$ is an involution on $\partial\tilde{A}(m, -\frac{3}{2})$, which will be defined in Section 3.

The following is a straightforward consequence of Theorem 1.1, 1.2 and [17].

Corollary 1.3.

(1) *There are no corks with special shadow complexity* 0.
(2) *A cork with special shadow complexity* 1 *is either $A(m, n)$ or $\tilde{A}(m, n-\frac{1}{2})$. In particular, there are infinitely many corks with shadow complexity* 1 *since there are infinitely many corks among $\tilde{A}(m, n-\frac{1}{2})$.*

Next we study Bing's house, which is a special polyhedron with two true vertices as shown in Figure 3. Bing's house was introduced by Bing in [9]. We denote it by B and let $B(l, m, n)$ be the compact oriented 4-manifold obtained by Turaev's reconstruction from B with gleams $\mathrm{gl}(e_3) = l, \mathrm{gl}(e_4) = m, \mathrm{gl}(e_5) = n$, where l, m, n are integers. For $B(l, m, n)$, we get the following.

Theorem 1.4.

(1) *If $|m| \geq 3$ and $|n| \geq 3$, then $B(l, m, n)$ is Mazur type.*
(2) *The pair $(B(0, m, n), f_{(m,n)})$ is a cork if m and n are negative.*

Here $f_{(m,n)}$ is an involution on $\partial B(0, m, n)$, which will be defined in Section 3.

Many corks W_n and $\overline{W}_n$ ($n \geq 1$) had been found by Akbulut and Yasui in [6]. It can be checked that the shadow complexities of W_n and $\overline{W}_n$ are at most $2n-1$ and $4n-2$ respectively. We can verify $A(1, -5) \cong \tilde{A}(-1, -\frac{3}{2}) \cong W_1$ and $B(0, -1, -1) \cong \overline{W}_1$ though we don't know if the other W_n's and $\overline{W}_n$'s appear in our corks or not.

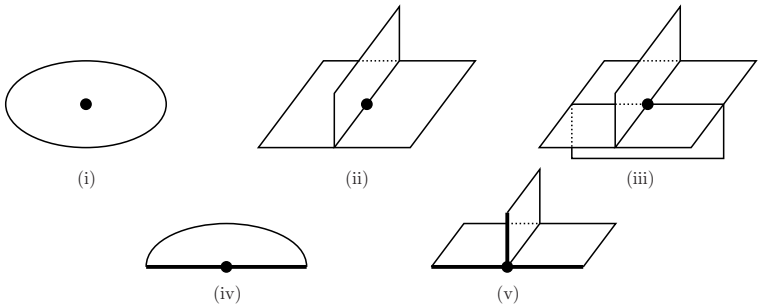

Figure 4. The local models of an almost-special polyhedron.

Main tool in the proofs is Kirby calculus. To distinguish topological types of $A(m,n)$'s and of $\tilde{A}(m,n-\frac{1}{2})$'s in Theorem 1.1 and 1.2 respectively, we compute the Casson invariants of their boundaries. To find corks among $\tilde{A}(m,n-\frac{1}{2})$ and $B(l,m,n)$, we check their Stein structures. The strategy is same as one used in [6].

In Section 2 we introduce the notions of shadows, Mazur manifolds, Stein surfaces and corks, and how to interpret from a Kirby diagram to a shadow. We give the proofs of our theorems in Section 3.

Acknowledgments. The author wishes to express his gratitude to his advisor, Masaharu Ishikawa, for encouragement and many useful suggestions. He also would like to thank the referee for helpful comments.

2. Preliminaries

Throughout this paper, we work in smooth category unless otherwise mentioned.

Let Y be a topological space, and X a subspace of Y. Assume that there exists a triangulations (L,K) of the pair (Y,X). By a *regular neighborhood* of X in Y we mean the underlying space of the star neighborhood of K in the barycentric subdivision of L. We denote it by $\mathrm{Nbd}(X;Y)$. We say that Y *collapses* onto X if there exists a triangulation (L_0,K_0) of (Y,X) such that L_0 collapses onto K_0.

2.1. **Shadows.** A compact topological space P is called an *almost-special polyhedron* if each point of P has a regular neighborhood which is homeomorphic to one of the five local models shown in Figure 4. A point whose regular neighborhood is of type (iii) is called a *true vertex*. We denote the set of true vertices by $V(P)$. The *singular set* of P is the set of points whose regular neighborhoods are of type (ii), (iii) or (v). We denote it by $Sing(P)$. The boundary ∂P of P is the set of points whose regular neighborhoods are of type (iv) or (v). Each component of $P \setminus Sing(P)$ is called a *region* of P. If a region R contains points of type (iv) then R is called a *boundary region*,

and otherwise it is called an *internal region*. Each region is a surface. If each region of P is homeomorphic to an open disk and any connected component of $Sing(P)$ contains at least one true vertex, then P is said to be *special*. Each connected component of $Sing(P) \setminus V(P)$ is called a *triple line*.

Definition 2.1. Let W be a compact oriented 4-manifold and let T be a (possibly empty) trivalent graph in the boundary ∂W of W. An almost-special polyhedron P in W is called a *shadow* of (W, T) if the following hold:

- W collapses onto P,
- P is locally flat in W, that is, for each point p of P there exists a local chart (U, ϕ) of W around p such that $\phi(U \cap P) \subset \mathbb{R}^3 \subset \mathbb{R}^4$ and
- $P \cap \partial W = \partial P = T$.

It is well-known that any compact oriented 4-manifold having a handle decomposition without 3- or 4-handles has a shadow [10].

Let R be an internal region of an almost-special polyhedron P and let $\bar{R}$ be a compact surface such that the interior of $\bar{R}$ is homeomorphic to R. The inclusion $i : R \to P$ can extend to a continuous map $\bar{i} : \bar{R} \to P$ such that $\bar{i}|_{\mathrm{Int}(\bar{R})}$ is injective and its image is the closure of R in P. For each point $x \in \bar{i}(\partial \bar{R})$, we can see that, locally, two regions are attached to $\bar{R}$ along $\partial \bar{R}$. Under this identification, for each boundary component of $\bar{R}$, there exists an immersed annulus or a Möbius band in $\mathrm{Nbd}(\bar{i}(\partial \bar{R}); P)$. Let N be the number of the Möbius bands as above. For each internal region R, we choose a half integer $\mathrm{gl}(R)$ such that the following holds:

$$\mathrm{gl}(R) - \frac{1}{2}N \in \mathbb{Z}.$$

We call $\mathrm{gl}(R)$ a *gleam* of R and the correspondence gl a *gleam* of P.

An almost-special polyhedron P endowed with a gleam is called an *integer shadowed polyhedron*, and denoted by (P, gl) (or simply P) .

Turaev showed that there exists a canonical mapping associating to an integer shadowed polyhedron (P, gl) a compact oriented smooth 4-manifold, denoted by M_P, in [28]. This is called *Turaev's reconstruction*. The method of this reconstruction is analogous to a process of attaching handles. Conversely, if a 4-manifold M has a shadow P then P can be equipped with the canonical gleam gl such that the 4-manifold M_P reconstructed from (P, gl) is diffeomorphic to M.

2.2. **Interpretation from a Kirby diagram to a shadow.** Now we introduce a method to obtain a shadow of a 4-manifold which is given by a Kirby diagram. We follow the method in [28, Chapter IX. 3.2.] and [10].

Let $\mathcal{D} = (\bigsqcup_{i=1}^{k} L_i^1) \amalg (\bigsqcup_{j=1}^{l} L_j^2) \subset S^3$ be a Kirby diagram, where L_i^1 $(i = 1, \ldots, k)$ is a dotted circle of a 1-handle and L_j^2 $(j = 1, \ldots, l)$ is a attaching circle of a 2-handle with framing coefficient n_j. We arbitrarily take

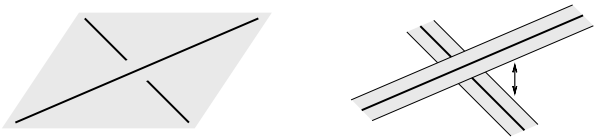

Figure 5. The first figure indicates a crossing point of a projection of a link component on an almost-special polyhedron. Then we can take the framing with respect to this almost-special polyhedron as in the second figure.

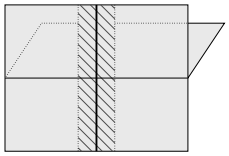

Figure 6. The framing is the hatched band.

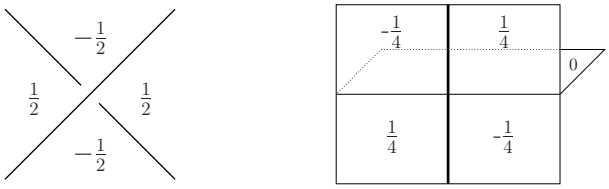

Figure 7. The local contributions to gleams: The left figure indicates the local contributions at s self-crossing point of C, and the right one indicates those at a crossing point of C and $Sing(Q)$.

an almost-special polyhedron Q in $S^3 \setminus (\bigsqcup_{i=1}^{k} L_i^1)$ such that $S^3 \setminus (\bigsqcup_{i=1}^{k} L_i^1)$ collapses onto Q. By isotopy in $S^3 \setminus (\bigsqcup_{i=1}^{k} L_i^1)$, we project $\bigsqcup_{j=1}^{l} L_j^2$ to $Q \setminus V(Q)$ such that each crossing point is a double point and not on $Sing(Q)$. We denote the image by $C = \bigcup_{j=1}^{l} C_j$. We then assign an over/under information to each crossing point such that the link restored from C according to the over/under information is isotopic to $\bigsqcup_{j=1}^{l} L_j^2$.

Definition 2.2.

(1) We call the *framing with respect to Q of C_j* an embedded annulus or Möbius band in S^3 obtained by taking a small regular neighborhood of C in Q and splitting it at each crossing point according to the over/under information as in Figure 5. Here if C runs over a triple line, we cut off the part which C does not lie from $\mathrm{Nbd}(C; Q)$ as in Figure 6.

(2) Let F_j be the framing with respect to Q of C_j. If F_j is an annulus, *the twist number of F_j* is defined by the linking number of the link $S^1 \amalg S^1 = \partial F_j \subset S^3$ whose orientations are chosen to be parallel. If F_j is a Möbius band, *the twist number of F_j* is defined by the half of the linking number of the link $S^1 \amalg S^1 = \partial F_j \amalg (\text{a core of } F_j) \subset S^3$ whose orientations are chosen to be parallel. We denote the twist number of F_j by $tw(C_j)$.

Let P be the almost-special polyhedron obtained from Q by attaching a disk D_j to each curve C_j along its boundary. Note that P is not necessarily embedded in S^3. We define the gleam gl of P in the following way.

- Let R be an internal region of P in the subdivision of Q by $C \cup Sing(Q)$. To four separated regions in a small regular neighborhood of each self-crossing point of C or each crossing point of C and the triple line of Q, we assign rational numbers as shown in Figure 7 (cf. [10, 28]). We define $\mathrm{gl}(R)$ by the sum of these local contributions for all crossing points of $C \cup Sing(Q)$ to which R is adjacent.
- The gleam of the region $\mathrm{Int}(D_j)$ is defined by $n_j - tw(C_j)$.

Thus we get an integer shadowed polyhedron (P, gl).

Lemma 2.3. *The 4-manifold reconstructed from* (P, gl) *is diffeomorphic to the 4-manifold given by the Kirby diagram* $\mathcal{D}$*.*

Proof. We only give a sketchy proof of this lemma. For details we refer the reader to [28] and [10]. We only verify that the gleam of the region R_j, which is the interior of D_j, is compatible with attaching the 2-handle. The framing of the 2-handle corresponding to L_j^2 is represented by a knot $\hat{L}_j^2$ parallel to L_j^2. Let B_j be an annulus whose boundaries are L_j^2 and $\hat{L}_j^2$. If B_j can embed in the framing F_j with respect to Q of C_j by isotopy sending L_j^2 to C_j, the gleam of R_j is 0 by [28]. Since the framing coefficient n_j is defined by $lk(L_j^2, \hat{L}_j^2)$ and the gleam of R_j increases by the number of the twists of B_j with respect to F_j, we conclude that the gleam of R_j is given by $n_j - tw(C_j)$. □

Note that, "the gleam of a boundary region" can be defined as above but it does not affect the reconstruction. Therefore, if the boundary region of P can collapse to the singular set $Sing(P)$, the resulting polyhedron is also a shadow of M_P. Two or more regions may be connected by this collapsing. In this case the gleam of the new region is given by the sum of the original gleams before connecting.

2.3. **Mazur manifolds and Akbulut's corks.**

Definition 2.4. A compact contractible 4-manifold which is not a 4-ball is called a *Mazur manifold* if it is obtained by attaching a 2-handle to $D^3 \times S^1$. If a Mazur manifold is not bounded by the 3-sphere then it is said to be *Mazur type*.

In [23], Mazur introduced Mazur manifolds $W^{\pm}(l, k)$, described in Figure 8, which were studied by Akbulut and Kirby in [3]. Remark that any compact contractible 4-manifold is bounded by a homology 3-sphere. In particular, if a shadow is contractible then its 4-manifold is also. Therefore such a 4-manifold always becomes a candidate of a Mazur manifold.

Now we introduce the definition of a *cork*, which was first found by Akbulut among Mazur manifolds in [1].

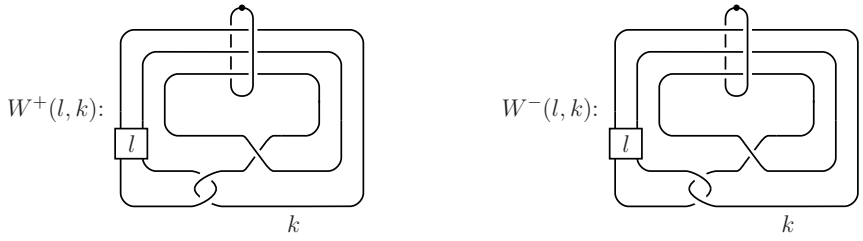

Figure 8. Kirby diagrams of the Mazur manifolds $W^{\pm}(l,k)$.

Definition 2.5. Let C be a contractible Stein domain and let $\tau : \partial C \to \partial C$ be an involution on the boundary of C. The pair (C, τ) is called a *cork* if τ extends to a self-homeomorphism on C, but can not extend to any self-diffeomorphism on C.

Here a *Stein manifold* is a complex manifold X such that X can be embedded into $\mathbb{C}^N$ by a proper holomorphic map. A compact 4-manifold W with boundary is called a *Stein domain* if there exists a Stein 4-manifold X with a plurisubharmonic function $f : X \to [0, \infty)$ and a regular value a of f such that $f^{-1}([0, a]) \cong W$.

Example 2.6. Akbulut and Yasui constructed many corks (W_n, f_n) $(n \geq 1)$ in [6]. Note that W_1 is just $W^-(0,0)$. They defined $f_n : \partial W_n \to \partial W_n$ by the involution obtained by first surgering $S^1 \times B^3$ to $B^2 \times S^2$ in the interior of W_n, and then surgering the other embedded $B^2 \times S^2$ back to $S^1 \times B^3$. We notice that the Kirby diagrams of W_n in [6] is a symmetric link, and the involution can be done by replacing the dot and " 0 " in the diagram.

Remark 2.7. We introduce an useful observation to detect a cork in [4] (cf. [2]). Let C be a compact oriented smooth 4-manifold whose Kirby diagram consists of a dotted unknot K_1 and a 0-framed unknot K_2 and assume that the following hold.

(1) The link $K_1 \amalg K_2$ is symmetric. Namely, the components K_1 and K_2 can be exchanged by isotopy in S^3.
(2) The linking number of K_1 and K_2 is ± 1.
(3) Exchange the notation of 1-handle to the ball notation. Then K_2 can be deformed to a Legendrian knot with respect to the standard contact structure on $\partial(D^4 \cup \text{1-handle}) = S^1 \times S^2$ such that the Thurston-Bennequin number is at least $+1$.

Let φ be the involution obtained by first surgering $S^1 \times B^3$ to $B^2 \times S^2$ in the interior of C, and then surgering the other embedded $B^2 \times S^2$ back to $S^1 \times B^3$. Then it is known that the pair (C, φ) is a cork, which is called *a cork of Mazur type* in [7].

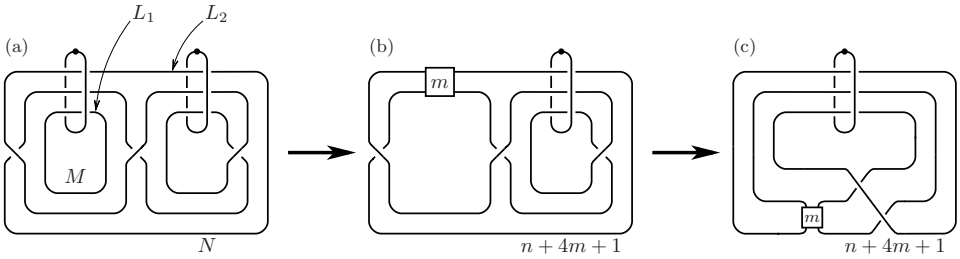

Figure 9. Kirby calculus in the proof of Lemma 3.1.

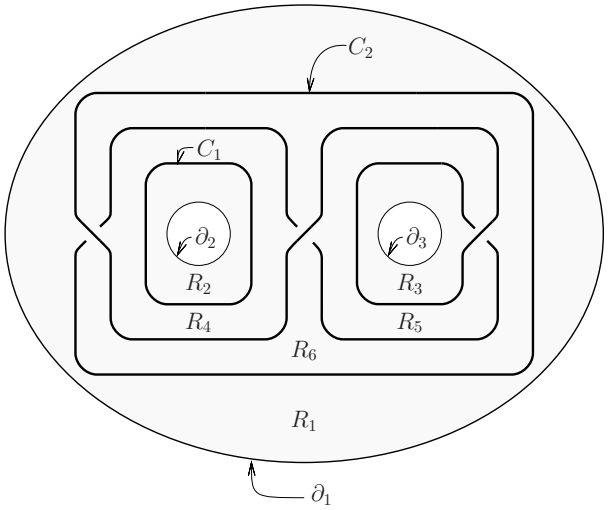

Figure 10. The pair of pants Q_A with immersed curves C_1 and C_2.

3. Proofs

This section separates into two parts. In the former part we give the proofs of Theorem 1.1 and 1.2, and we give the proof of Theorem 1.4 in the latter part.

3.1. **The case of** 1 **true vertex.**

Lemma 3.1. *The 4-manifold $A(m,n)$ is represented by the Kirby diagram shown in Figure 9 (c).*

Proof. Consider the pair of pants Q_A shown in Figure 10, where ∂_1, ∂_2 and ∂_3 are its boundary components, and C_1 and C_2 are immersed curves on Q_A equipped with over/under information at each double point. We note that the pair of pants Q_A is divided into 6 regions $R_1, \ldots, R_6$ by C_1 and C_2.

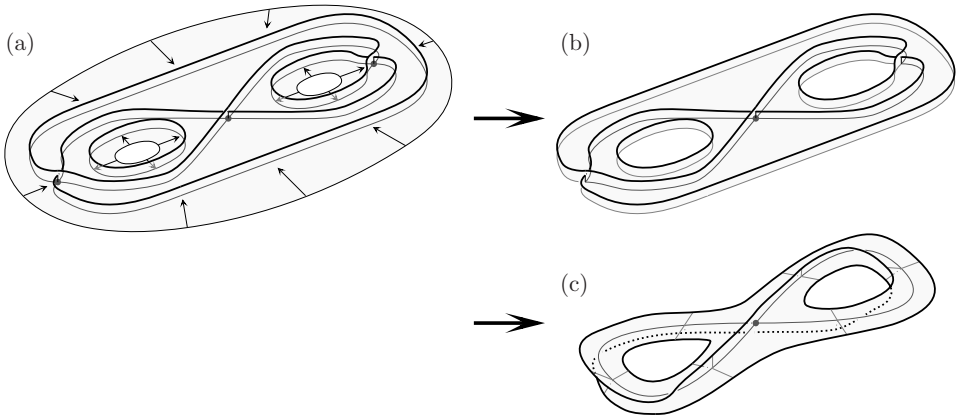

Figure 11. The almost-special polyhedron obtained from Q_A by attaching two annuli along their boundaries to C_1 and C_2 is described in (a). This can collpase into another one shown in (b) as indicated by the arrows in (a). The resulting polyhedron can be embedded into R^3 as shown in (c).

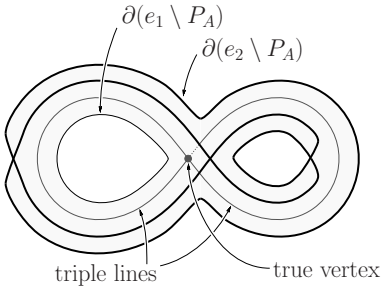

Figure 12. The almost-special polyhedron P_A. A similar figure can be seen in [19, Figure 27(i)].

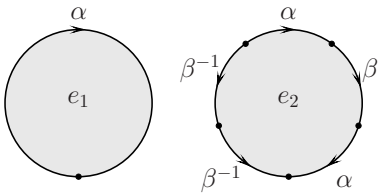

Figure 13. A cell decomposision of A.

We next consider the almost-special polyhedron obtained from Q_A by attaching two annuli along their boundaries to C_1 and C_2, as shown in Figure 11 (a). By collapsing along the boundary regions R_1, R_2, R_3 as indicated by the arrows in the figure, it becomes a new almost-special polyhedron, denoted by P_A, as shown in Figure 11 (b). We note that these figures are described as immersed in $\mathbb{R}^3$. In fact the polyhedron P_A can be emdedded in $\mathbb{R}^3$ as shown in Figure 11 (c) and it is homeomorphic to a regular neighborhood of $Sing(A)$ in A. We note that P_A is also described as shown in Figure 12. The above fact can be verified by seeing how the regions are glued along the singular set. As in Ikeda [17, Fig 8.(i)], the polyhedron A is decomposed into two regions as shown in Figure 13.

Let Q'_A be the almost-special polyhedron obtained from Q_A by attaching two disks D_1 and D_2 to C_1 and C_2 along the boundaries respectively. From the above observation, it follows that the almost-special polyhedron obtained from Q'_A by collapsing along the three boundary regions R_1, R_2, R_3 is homeomorphic to A. Under this identification, we have $e_1 = D_1 \cup R_4$ and $e_2 = D_2 \cup R_5 \cup R_6$.

We next consider the Kirby diagram shown in Figure 9 (a), where L_1 and L_2 are attaching circles of 2-handles, whose framing coefficients are represented by M and N respectively. We can see that Q_A can be embedded in the Kirby diagram in Figure 9 (a) such that $S^3 \setminus$ (dotted circles) collapses to Q_A and L_1 and L_2 are projected onto C_1 and C_2 respectively. We can also see that the 4-manifold given by Figure 9 (a) has a shadow Q'_A, and then also A.

What is left is to compute the relation between M, N and gleams $m = \mathrm{gl}(e_1), n = \mathrm{gl}(e_2)$. Let F_i $(i = 1, 2)$ be the framing with respect to Q_A of C_i. Both F_1 and F_2 are annuli and their twist numbers are $tw(C_1) = 0$ and $tw(C_2) = 1$. Therefore,

$$\mathrm{gl}(D_1) = M - tw(C_1) = M$$
$$\mathrm{gl}(D_2) = N - tw(C_2) = N - 1$$

by Lemma 2.3. By the local contributions to gleams as in Figure 7, we have

$$\mathrm{gl}(R_4) = 1 \cdot \frac{1}{2} + 1 \cdot (-\frac{1}{2}) = 0$$
$$\mathrm{gl}(R_5) = 1 \cdot \frac{1}{2} + 2 \cdot (-\frac{1}{2}) = -\frac{1}{2}$$
$$\mathrm{gl}(R_6) = 3 \cdot \frac{1}{2} + 2 \cdot (-\frac{1}{2}) = \frac{1}{2}.$$

We recall the earlier-mentioned identifications: $e_1 = D_1 \cup R_4$ and $e_2 = D_2 \cup R_5 \cup R_6$. Considering the changes of the gleams after collapsing along the boundary regions R_1, R_2, R_3, we have

$$\mathrm{gl}(e_1) = \mathrm{gl}(D_1) + \mathrm{gl}(R_4),$$
$$\mathrm{gl}(e_2) = \mathrm{gl}(D_2) + \mathrm{gl}(R_5) + \mathrm{gl}(R_6).$$

Hence $M = m$ and $N = n + 1$. Thus we get the Kirby diagram of $A(m, n)$ in Figure 9 (a). Since the pair of the left 1-handle and the 2-handle corresponding to L_1 is a canceling pair, we can erase this pair and get Figure 9 (b). By isotopy, we get the Kirby diagram of $A(m, n)$ as in Figure 9 (c). □

Lemma 3.2. *There exists a sequence of Kirby moves from the left to the right in Figure 14 for any m, where the tangle d satisfies the following properties:*

1. *the linking number of the link shown in Figure 15 is $|m|$ and*
2. *the link component with framing coefficient ε in Figure 14 is an unknot,*

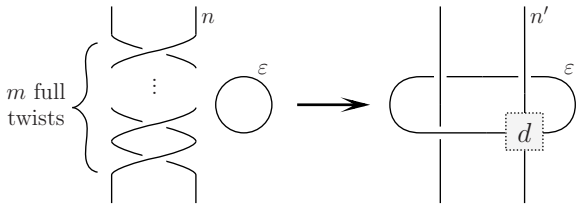

Figure 14. Kirby moves in Lemma 3.2.

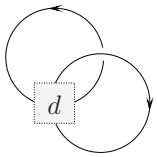

Figure 15. The link in Lemma 3.2.

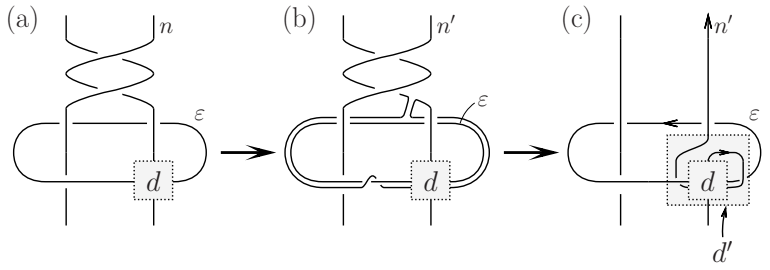

Figure 16. The proof of the case $m > 0$.

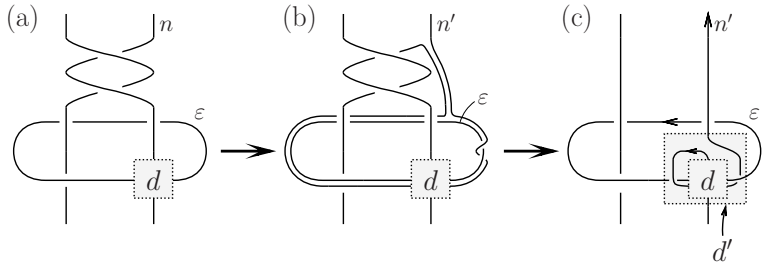

Figure 17. The proof of the case $m < 0$.

where $\varepsilon = -1$ *if* $m > 0$ *and* $\varepsilon = +1$ *if* $m < 0$.

Proof. We first prove for the case $m > 0$ by induction on m. It is easy for $m = 1$.

See Figure 16. We assume that this lemma holds for m and prove it for $m+1$. We slide the 2-handle and get Figure 16 (b). The isotopy gives Figure 16 (c). Since the link component with framing coefficient ε is not moved, it is still an unknot. Let d' be the tangle shown in Figure 16 (c). In Figure 16 (b) and (c), the link component with framing coefficient n' intersects the vertical sides of the tangle d and is running parallel to the other strand with framing coefficient ε inside of d. Note that these two parallel strands in d have no crossing because of the condition (2). Hence there is no change of

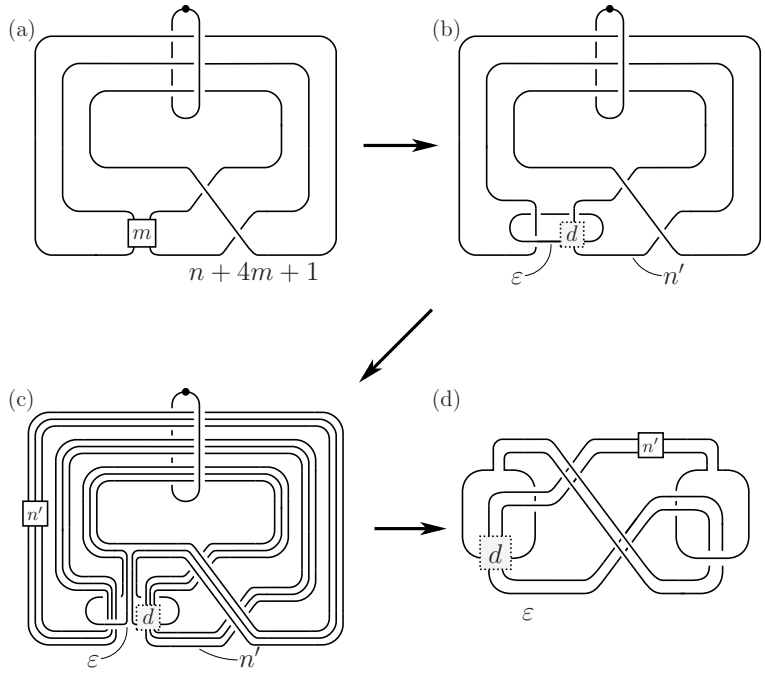

Figure 18. Kirby calculus in the proof of Theorem 1.1.

crossing number in d. On the other hand, out of d in d', we can see two positive crossings. Then computing the linking number of the link obtained by setting d' instead of the tangle d in Figure 15, we get $m+1$.

The proof for the case $m < 0$ is similar. See Figure 17. □

Proof of Theorem 1.1. The 4-manifold $A(m,n)$ is contractible since A is contractible. By the Kirby diagram in Figure 9 (c), $A(m,n)$ satisfies the condition of the handle decomposition for a Mazur manifold. We will compute the Casson invariant of the boundary of $A(m,n)$ to verify whether $A(m,n)$ is Mazur type.

Let us blow-up and apply Lemma 3.2 to the diagram shown in Figure 18 (a), and we get Figure 18 (b). Sliding the 2-handle with framing coefficient ε another 2 times, we get Figure 18 (c). We erase the canceling pair and get Figure 18 (d). Now we focus on the boundary of $A(m,n)$ and regard Figure 3.2 (d) as a surgery diagram of $\partial A(m,n)$. Note that the two strands in the tangle d, intersecting two horizontal sides of d, are parallel. Moreover, the strand in the tangle d, intersecting two vertical sides of d has no self-intersection. Hence the knot in Figure 18 (d) is a ribbon knot. We denote this knot by $K_{(m,n)}$. Next we compute the Alexander polynomial of $K_{(m,n)}$ by using the method in [27], in which Terasaka computed the Alexander

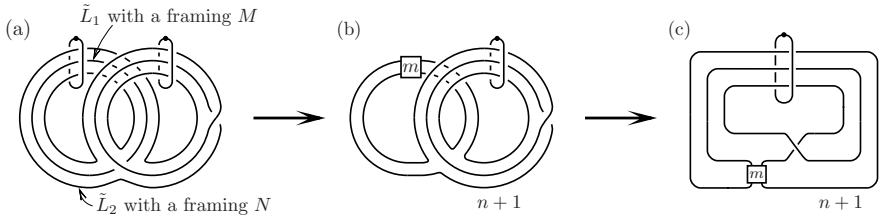

Figure 19. Kirby calculus in the proof of Lemma 3.3.

polynomials of ribbon knots. We get

$$\Delta_{K_{(m,n)}}(t) = t^{|m|+1} - t^{|m|} - t + 3 - t^{-1} - t^{-|m|} + t^{-|m|-1}.$$

Then the Casson invariant of $\partial A(m,n)$ can be computed by using the surgery formula for the Casson invariant as follows:

$$\begin{aligned}\lambda(\partial A(m,n)) &= \lambda(S^3 + \frac{1}{\varepsilon}\cdot K_{(m,n)}) \\ &= \lambda(S^3) + \frac{\varepsilon}{2}\Delta''_{K_{(m,n)}}(1) \\ &= 0 + \frac{\varepsilon}{2}\cdot 4|m| \\ &= -2m.\end{aligned}$$

Hence $\partial A(m,n)$ is not homeomorphic to S^3 for $m \neq 0$, and $A(m,n)$'s are mutually not homeomorphic for different m. □

Next we study the compact oriented 4-manifold $\tilde{A}(m, n-\frac{1}{2})$ whose shadow is $\tilde{A}$. We first describe $\tilde{A}(m, n-\frac{1}{2})$ by the Kirby diagram to prove Theorem 1.2.

Lemma 3.3. *The 4-manifold $\tilde{A}(m, n-\frac{1}{2})$ is represented by the Kirby diagram shown in Figure 19 (c).*

Proof. The proof is similar to Lemma 3.1. Let $Q_{\tilde{A}}$ be a once-punctured torus with immersed curves $\tilde{C}_1$ and $\tilde{C}_2$ on it as shown in Figure 20. we note that the curves are equipped with over/under information at each double point and $Q_{\tilde{A}}$ is divided into two regions R_7, R_8 by $\tilde{C}_1$ and $\tilde{C}_2$.

As we observed in the proof of Lemma 3.1, a regular neighborhood of $Sing(\tilde{A})$ in $\tilde{A}$ can be obtained from $Q_{\tilde{A}}$ by attaching annuli and collapsing. First we attach two annuli along their boundaries to $\tilde{C}_1$ and $\tilde{C}_2$, and then let it collapse along the boundary region R_7. The resulting polyhedron is homeomorphic to $\mathrm{Nbd}(Sing(\tilde{A}); \tilde{A})$, which is shown in Figure 21. It can be checked by seeing how the regions are glued along the singular set. See Figure 2.

Let $Q'_{\tilde{A}}$ be the almost-special polyhedron obtained from $Q_{\tilde{A}}$ by attaching two disks $\tilde{D}_1$ and $\tilde{D}_2$ to $\tilde{C}_1$ and $\tilde{C}_2$ along the boundaries respectively. It can

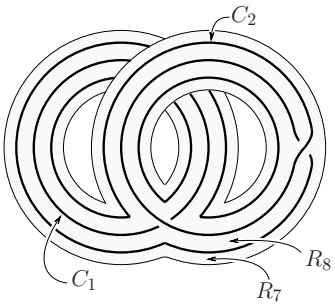

Figure 20. The once-punctured torus $Q_{\tilde{A}}$ and immersed curves $\tilde{C}_1$ and $\tilde{C}_2$.

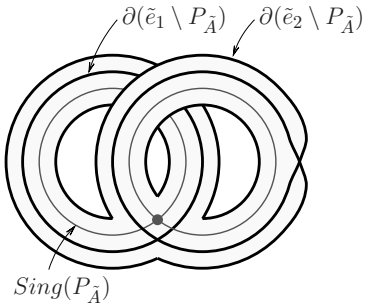

Figure 21. The almost-special polyhedron $P_{\tilde{A}}$.

be seen that the almost-special polyhedron obtained from $Q'_{\tilde{A}}$ by collapsing along the boundary region R_7 is homeomorphic to $\tilde{A}$. Note that $\tilde{e}_1 = \tilde{D}_1$ and $\tilde{e}_2 = \tilde{D}_2 \cup R_8$ under this identification.

Next we consider the Kirby diagram shown in Figure 19 (a). In the figure, $\tilde{L}_1$ and $\tilde{L}_2$ are attaching circles of 2-handles, whose framing coefficients are represented by M and N as in the figure respectively. We can see that $Q_{\tilde{A}}$ can be embedded in the Kirby diagram in Figure 19 (a) such that $S^3 \setminus$ (dotted circles) collapses to $Q_{\tilde{A}}$ and $\tilde{L}_1$ and $\tilde{L}_2$ are projected onto $\tilde{C}_1$ and $\tilde{C}_2$ respectively. We can also see that the 4-manifold given by Figure 19 (a) has a shadow $Q'_{\tilde{A}}$ and also $\tilde{A}$.

Let $\tilde{F}_i$ $(i = 1, 2)$ be the framing with respect to $Q_{\tilde{A}}$ of $\tilde{C}_i$. Both $\tilde{F}_1$ and $\tilde{F}_2$ are annuli, and we get the twist numbers $tw(\tilde{C}_1) = 0$ and $tw(\tilde{C}_2) = 1$. Therefore, by Lemma 2.3

$$\mathrm{gl}(\tilde{D}_1) = M - tw(\tilde{C}_1) = M$$
$$\mathrm{gl}(\tilde{D}_2) = N - tw(\tilde{C}_2) = N - 1.$$

By the local contributions to gleams as in Figure 7, we have

$$\mathrm{gl}(R_8) = 3 \cdot \frac{1}{2} + 4 \cdot (-\frac{1}{2}) = -\frac{1}{2}.$$

We recall that $\tilde{e}_1 = \tilde{D}_1$ and $\tilde{e}_2 = \tilde{D}_2 \cup R_8$. Considering the changes of the gleams by collapsing along R_7, we have

$$\mathrm{gl}(\tilde{e}_1) = \mathrm{gl}(\tilde{D}_1),$$
$$\mathrm{gl}(\tilde{e}_2) = \mathrm{gl}(\tilde{D}_2) + \mathrm{gl}(R_8).$$

Hence $M = m$ and $N = n+1$. Thus we get the Kirby diagram of $\tilde{A}(m, n-\frac{1}{2})$. We erase the canceling pair and get Figure 19 (b). By isotopy, we get Figure 19 (c). □

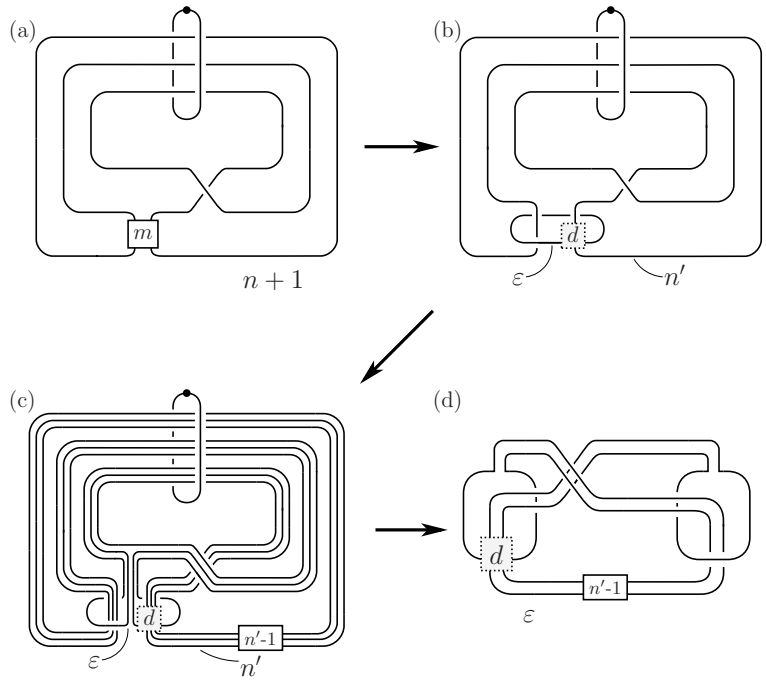

Figure 22. Kirby calculus in the proof of Theorem 1.2.

Remark 3.4. It is easy to check that $A(\pm 1, n) \cong \tilde{A}(\mp 1, n \pm \frac{7}{2})$ by isotopies in their Kirby diagrams. We don't know whether or not there are other diffeomorphisms between $A(m, n)$ and $\tilde{A}(m', n' - \frac{1}{2})$.

We now define

$$\tilde{f}_m : \partial \tilde{A}(m, -\frac{3}{2}) \to \partial \tilde{A}(m, -\frac{3}{2})$$

by the involution obtained by first surgering $S^1 \times B^3$ to $B^2 \times S^2$ in the interior of $\tilde{A}(m, -\frac{3}{2})$, then surgering the other embedded $B^2 \times S^2$ back to $S^1 \times B^3$. We notice the Kirby diagram of $\tilde{A}(m, n - \frac{1}{2})$ in Figure 19 (c) is a symmetric link, and the involution can be done by replacing the dot and " 0 " in the diagram.

Proof of Theorem 1.2. (1) The proof is similar to Theorem 1.1. First the 4-manifold $\tilde{A}(m, n - \frac{1}{2})$ is contractible since $\tilde{A}$ is contractible. By the Kirby diagram, $\tilde{A}(m, n - \frac{1}{2})$ has a handle decomposition satisfying the condition for a Mazur manifold.

We next compute the Casson invariant of the boundary of $\tilde{A}(m, n - \frac{1}{2})$. Let us blow-up and apply Lemma 3.2 to the diagram as shown in Figure 22 (a), and we get Figure 22 (b). We slide the 2-handle with framing coefficient ε another 2 times, and we get Figure 22 (c). We erase the canceling pair

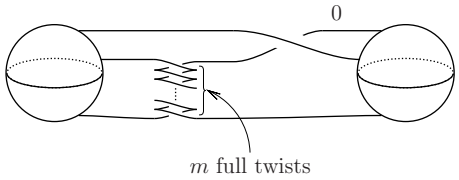

Figure 23. The attaching circle of the 2-handle of $\tilde{A}(m,-\frac{3}{2})$ in Legendrian position.

and get Figure 22 (d). We notice the knot in Figure 22 (d) is a ribbon knot. We denote this knot by $\tilde{K}_{(m,n)}$. By using the method in [27] again, we get

$$\Delta_{\tilde{K}_{(m,n)}}(t) = -t^{|m|} + t^{|m|-1} - t + 3 - t^{-1} + t^{-|m|+1} - t^{-|m|}.$$

Then the Casson invariant of $\partial\tilde{A}(m,n-\frac{1}{2})$ can be computed by using the surgery formula for the Casson invariant as follows:

$$\begin{aligned}\lambda(\partial\tilde{A}(m,n-\frac{1}{2})) &= \lambda(S^3 + \frac{1}{\varepsilon}\cdot\tilde{K}_{(m,n)}) \\ &= \lambda(S^3) + \frac{\varepsilon}{2}\Delta''_{\tilde{K}_{(m,n)}}(1) \\ &= 0 - \frac{\varepsilon}{2}\cdot 4|m| \\ &= 2m.\end{aligned}$$

Hence $\partial\tilde{A}(m,n-\frac{1}{2})$ is not homeomorphic to S^3 for $m \neq 0$, and $\tilde{A}(m,n-\frac{1}{2})$'s are mutually not homeomorphic for different m.
(2) Set $n=-1$ and $m<0$. To show that $(\tilde{A}(m,-\frac{3}{2}),\tilde{f}_m)$ is a cork, we use the notion in Remark 2.7. By Lemma 3.3, it is easy to check that $\tilde{A}(m,-\frac{3}{2})$ has a Kirby diagram consisting of a dotted unknot and 0-framed unknot such that the link is symmetric and its linking number is ± 1. Therefore, it remains only to check the condition of the Thurston-Bennequin number. Deform the attaching circle of the 2-handle in the Kirby diagram of $\tilde{A}(m,-\frac{3}{2})$ to a Legendrian knot with respect to the canonical contact structure on $S^1\times S^2$ as shown in Figure 23 (in which we denote the 1-handle by 3-balls instead of dotted circle notation). Then we get its Thurston-Bennequin number as

$$tb = wr - \sharp\{\text{left cusps}\} = (2|m|+1) - (2|m|-1) = 2.$$

Thus we are done.

□

We recall the definition of the (special) shadow complexity of a 4-manifold.

Definition 3.5. (1) If M admits a handle decomposition without 3- or 4-handles, its (*special*) *shadow complexity* is defined by the minimal number of true vertices among all (special) shadows of M.

(2) If M admits no handle decomposition without 3- or 4-handles, its (*special*) *shadow complexity* is defined by the minimal number of (special) shadow complexities of 4-manifolds to which we can attach 3- and 4-handles such that the resulting manifold are diffeomorphic to M.

Proof of Corollary 1.3. By [17], there are no acyclic special polyhedra without true vertices, and acyclic special polyhedra with only one true vertex are just A and $\tilde{A}$. A cork is defined as a Stein domain, which admits a handle decomposition without 3- or 4-handles [16]. Thus there are no corks with special shadow complexity 1 other than $A(m,n)$ or $\tilde{A}(m,n-\frac{1}{2})$. □

Now we compare our results and previous works.

Corollary 3.6. *For any integers l and k, $W^{\pm}(l,k) \cong \tilde{A}(\pm 1, l+k-\frac{3}{2})$ holds.*

Proof. Set $m = \pm 1$ and $n = k-1$ in the Kirby diagram of $\tilde{A}(m,n-\frac{1}{2})$ shown in Figure 19 (c), and we get $W^{\pm}(0,k) \cong \tilde{A}(\pm 1, k-\frac{3}{2})$. Akbulut and Kirby showed $W^{\pm}(l,k) \cong W^{\pm}(l+1,k-1)$ in [3], and then $W^{\pm}(l,k) \cong W^{\pm}(0,l+k) \cong \tilde{A}(\pm 1, l+k-\frac{3}{2})$. □

Remark 3.7. If (P,gl) is a shadow of a 4-manifold M, then the 4-manifold constructed from the pair $(P,-\mathrm{gl})$ is diffeomorphic to $-M$, where $-\mathrm{gl}$ is the gleam gl with the opposite sign. We apply this as follows:

$$\begin{aligned} W^{-}(l,k) \cong & \tilde{A}(-1, l+k-\frac{3}{2}) \\ \cong & -\tilde{A}(1, -l-k+\frac{3}{2}) \\ = & -\tilde{A}(1, (-l+2)+(-k+1)-\frac{3}{2}) \\ \cong & -W^{+}(-l+2, -k+1). \end{aligned}$$

Hence $W^{-}(l,k) \cong -W^{+}(-l+2,-k+1)$. Note that this assertion has been proven by Akbulut and Kirby in [3]. Their proof is done by Kirby calculus.

The following is a corollary of Remark 3.4.

Corollary 3.8. *For any integers l and k, $W^{-}(l,k) \cong A(1, l+k-5)$ and $W^{+}(l,k) \cong A(-1, l+k+2)$ hold.*

3.2. **The case of 2 true vertices.** Next we study the compact oriented 4-manifold $B(l,m,n)$ whose shadow is Bing's house B. We first describe $B(l,m,n)$ by the Kirby diagram and then prove Theorem 1.2.

Lemma 3.9. *The 4-manifold $B(l,m,n)$ is represented by the Kirby diagram shown in Figure 24 (c).*

Proof. The proof is similar to Lemma 3.1 and 3.3. Let Q_B be a twice-punctured torus with immersed curves C_3, C_4, C_5 equipped with over/under

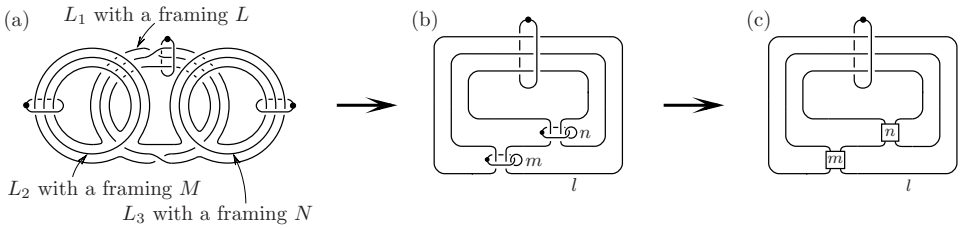

Figure 24. Kirby calculus in the proof of Lemma 3.9.

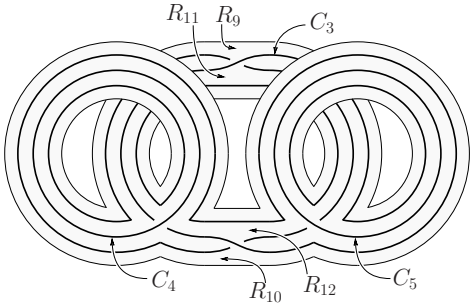

Figure 25. The twice-punctured torus Q_B and immersed curves C_3, C_4 and C_5.

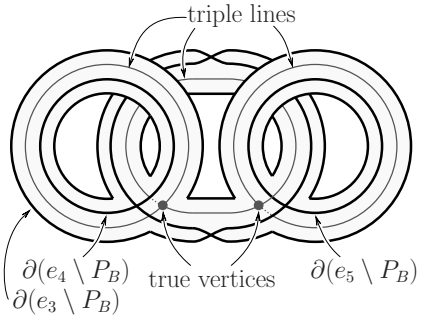

Figure 26. The almost-special polyhedron P_B.

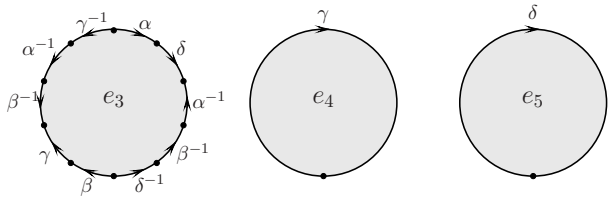

Figure 27. A cell decomposition of B.

information at each double point, as shown in Figure 25. Note that C_3, C_4 and C_5 divide Q_B into 4 regions $R_9, \ldots, R_{12}$.

A regular neighborhood of $Sing(B)$ in B can be obtained from Q_B by first attaching three annuli along their boundaries to C_3, C_4, C_5 and then collapsing along the boundary region R_9 and R_{10}. It is shown in Figure 26. As in Ikeda [18, Fig 4.], B decomposes as shown in Figure 27.

Let Q'_B be the almost-special polyhedron obtained from Q_B by attaching three disks D_3, D_4 and D_5 to C_3, C_4 and C_5 along the boundary respectively. It is easy to check that the almost-special polyhedron obtained from Q'_B by

collapsing along the boundary regions R_9 and R_{10} is homeomorphic to B. Note that $e_3 = D_3 \cup R_{11} \cup R_{12}$, $e_4 = D_4$ and $e_5 = D_5$ under this identification.

Next we consider the Kirby diagram shown in Figure 24 (a). In the figure, L_3, L_4 and L_5 are attaching circles of 2-handles, whose framing coefficients are represented by L, M and N as in the figure respectively. We can see that Q_B can be embedded in the Kirby diagram in Figure 24 (a) such that $S^3 \backslash$(dotted circles) collapses to Q_B and L_i is projected onto C_i for $i = 3, 4, 5$. We can also see that the 4-manifold given by Figure 24 (a) has a shadow Q'_B, and then also B.

Let F_i $(i = 3, 4, 5)$ be the framing with respect to Q_B of C_i. Each F_i is an annulus. We get the twist number $tw(C_i) = 0$ for each $i = 3, 4, 5$. By Lemma 2.3, we have

$$\begin{aligned} \mathrm{gl}(D_3) &= L - tw(C_3) = L \\ \mathrm{gl}(D_4) &= M - tw(C_4) = M \\ \mathrm{gl}(D_5) &= N - tw(C_5) = N. \end{aligned}$$

By the local contributions to gleams as in Figure 7, we have

$$\begin{aligned} \mathrm{gl}(R_{11}) &= 4 \cdot \frac{1}{2} + 3 \cdot (-\frac{1}{2}) = \frac{1}{2} \\ \mathrm{gl}(R_{12}) &= 3 \cdot \frac{1}{2} + 4 \cdot (-\frac{1}{2}) = -\frac{1}{2}. \end{aligned}$$

We recall that $e_3 = D_3 \cup R_{11} \cup R_{12}$, $e_4 = D_4$ and $e_5 = D_5$, and we have

$$\begin{aligned} \mathrm{gl}(e_3) &= \mathrm{gl}(D_3) + \mathrm{gl}(R_{11}) + \mathrm{gl}(R_{12}), \\ \mathrm{gl}(e_4) &= \mathrm{gl}(D_4), \\ \mathrm{gl}(e_5) &= \mathrm{gl}(D_5). \end{aligned}$$

Hence $L = l, M = m$ and $N = n$. Thus we get the Kirby diagram of $B(l, m, n)$. By isotopy, we get Figure 24 (b). We erase the canceling pairs and get Figure 24 (c). □

We now define

$$f_{(m,n)} : \partial B(0, m, n) \to \partial B(0, m, n)$$

by the involution obtained by first surgering $S^1 \times B^3$ to $B^2 \times S^2$ in the interior of $B(0, m, n)$, then surgering the other embedded $B^2 \times S^2$ back to $S^1 \times B^3$. We notice the Kirby diagram of $B(l, m, n)$ is a symmetric link, and the involution can be done by replacing the dot and " 0 " in the diagram.

Proof of Theorem 1.4. (1) Bing's house is a special polyhedron, that is, each region is a disk. By Turaev's reconstruction, the 4-manifold $B(l, m, n)$ is obtained from $\natural 3 S^1 \times D^3$ by attaching three 2-handles correspomding to the regions e_3, e_4 and e_5. Let L be the attaching link of these 2-handles in $\partial(\natural 3 S^1 \times D^3) = \sharp 3 S^1 \times S^2$. As in Costantino and Thurston [14, Proposition 3.33], the complement of L in $\sharp 3 S^1 \times S^2$ has a complete finite volume

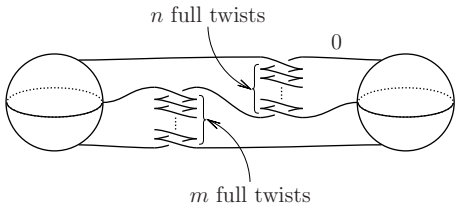

Figure 28. The attaching circle of the 2-handle of $B(0,m,n)$ in Legendrian position.

hyperbolic structure. Hence the boundary of $B(l,m,n)$ may have a hyperbolic structure by Dehn filling $(\sharp 3S^1 \times S^2) \setminus L$ suitably. The slope length of the Dehn filling corresponding to each region of a special polyhedron as follows. Let R be a region of a special polyhedron P. The slope length $\mathrm{sl}(R)$ corresponding to R is given by $\sqrt{4\mathrm{gl}(R)^2 + k(R)^2}$, where $k(R)$ is the number of times R is adjacent to the true vertices of P with multiplicity (cf. Ishikawa and Koda [19, Lemma 5.3]). In our case, the values of sl's on the three regions are

$$\mathrm{sl}(e_3) = \sqrt{4\mathrm{gl}(e_3)^2 + k(e_3)^2} = \sqrt{4l^2 + 100},$$
$$\mathrm{sl}(e_4) = \sqrt{4\mathrm{gl}(e_4)^2 + k(e_4)^2} = \sqrt{4m^2 + 1},$$
$$\mathrm{sl}(e_5) = \sqrt{4\mathrm{gl}(e_5)^2 + k(e_5)^2} = \sqrt{4n^2 + 1}.$$

Note that, from Figure 27, $k(e_3) = 10$ and $k(e_4) = k(e_5) = 1$. If $|m|, |n| \geq 3$, these values $\mathrm{sl}(e_3), \mathrm{sl}(e_4)$ and $\mathrm{sl}(e_5)$ are greater than 6. Then the boundary of $B(l,m,n)$ has a hyperbolic structure by the 6-Theorem, due to Agol [8, Theorem 6.2] and Lackenby [20, Theorem 3.1], and the Geometrization theorem by Perelman [24, 25, 26]. Since Bing's house is contractible, $B(l,m,n)$ is contractible. $B(l,m,n)$ satisfies the condition of a handle decomposition of a Mazur manifold by the Kirby diagram shown in Figure 24 (c). Hence $B(l,m,n)$ is Mazur type.

(2) The proof is similar to the proof of Theorem 1.2 (cf. Remark 2.7). Set $l = 0$ and $m, n < 0$. The Kirby diagram of $B(0,m,n)$ in Figure 24 (c) consists of a dotted unknot and 0-framed unknot such that the link is symmetric and its linking number is ± 1. Let us deform the attaching circle of $B(0,m,n)$ to a Legendrian knot with respect to the canonical contact structure on $S^1 \times S^2$ as shown in Figure 28 (in which we adopt the ball notation for the 1-handle). Then we can get the Thurston-Bennequin number

$$tb = wr - \sharp\{\text{left cusps}\} = (2|m| + 2|n|) - ((2|m| - 1) + (2|n| - 1)) = 2.$$

By Remark 2.7, the proof is now completed.

□

Corollary 3.10. *If m and n are the same sign, then $B(0,m,n)$ is Mazur type.*

Proof. Suppose $m, n < 0$. If $\partial B(0, m, n) \cong S^3$, then $f_{(m,n)}$ is isotopic to the identity. Hence $f_{(m,n)}$ extend to a self-diffeomorphism of $B(0, m, n)$ as the identity map. This is a contradiction since $B(0, m, n)$ is a cork. Therefore $B(0, m, n)$ is Mazur type.

If $m, n > 0$, since

$$\partial B(0, m, n) \cong \partial(-B(0, -m, -n)) \cong -\partial(B(0, -m, -n)),$$

the assertion holds by the same argument. □

Remark 3.11. The 4-manifold $B(0, -1, -1)$ is diffeomorphic to $\overline{W}_1$, which is a cork introduced by Akbulut and Yasui in [6].

References

[1] S. Akbulut: *A Fake compact contractible 4-manifold*, J. Diff. Geom. **33** (1991), 335–356.

[2] S. Akbulut and Ç. Karakurt: *Action of the cork twist on Floer homology*, Proceedings of the Gökova Geometry-Topology Conference 2011, 42-52, Int. Press, Somerville, MA, 2012.

[3] S. Akbulut and R. Kirby: *Mazur manifolds*, Michigan Math. J. **26** (1979), 259–284.

[4] S. Akbulut and R. Matveyev: *Exotic structures and adjunction inequality*, Turkish J. Math. **21** (1997), no. 1, 47–53

[5] S. Akbulut and R. Matveyev: *A convex decomposition theorem for 4-manifolds*, Internat. Math. Res. Notices 1998, no. 7, 371–381.

[6] S. Akbulut and K. Yasui: *Corks, Plugs and exotic structures*, Journal of Gökova Geometry Topology **2** (2008), 40–82.

[7] S. Akbulut and K. Yasui: *Stein 4-manifolds and corks*, Journal of Gökova Geometry Topology. GGT **6** (2012), 58–79.

[8] I. Agol: *Bounds on exceptional Dehn filling*, Geom. Topol. **4** (2000), 431-449.

[9] R.H. Bing: *Some aspects of the topology of 3-manifolds related to the Poincare conjecture*, in Lectures on Modern Mathematics II (T. L. Saaty, ed.), Wiley, New York, 1964.

[10] F. Costantino: Shadows and branched shadows of 3 and 4-manifolds, Scuola Normale Superiore, Edizioni della Normale, Pisa, Italy, 2005.

[11] F. Costantino: *Complexity of 4-manifolds*, Experiment. Math. **15** (2006), no. 2, 237–249.

[12] F. Costantino: *Stein domains and branched shadows of 4-manifolds*, Geom. Dedicata **121** (2006), 89–111.

[13] F. Costantino: *Branched shadows and complex structures of 4-manifolds*, J. Knot Theory Ramifications **17** (2008), no. 11, 1429–1454.

[14] F. Costantino and D. Thurston: *3-manifolds efficiently bound 4-manifolds*, J. Topol. **1** (2008), no. 3, 703–745.

[15] C. Curtis, M. Freedman, W. C. Hsiang and R. Stong: *A decomposition theorem for h-cobordant smooth simply-connected compact 4-manifolds*, Invent. Math. **123** (1996), no. 2, 343–348.

[16] Y. Eliashberg: *Topological characterization of Stein manifolds of dimension > 2*, Internat. J. Math. **1** (1990), no. 1, 29–46.

[17] H. Ikeda: *Acyclic fake surfaces*, Topology **10** (1971), 9–36.

[18] H. Ikeda: *Acyclic fake surfaces which are spines of 3-manifolds*, Osaka J. Math. **9** (1972), 391–408.

[19] M. Ishikawa and Y. Koda: *Stable maps and branched shadows of 3-manifolds*, Math. Ann. **367** (2017), 1819–1863.

[20] M. Lackenby: *Word hyperbolic Dehn surgery*, Invent. Math. **140** (2000), no. 2, 243–282.
[21] B. Martelli: *Four-manifolds with shadow-complexity zero*, Int. Math. Res. Not. IMRN **2011**, 1268–1351.
[22] R. Matveyev: *A decomposition of smooth simply-connected h-cobordant 4-manifolds*, J. Diff. Geom. **44** (1996), no. 3, 571–582.
[23] B. Mazur: *A note on some contractible 4-manifolds*, Ann. of Math. (2) **73** (1961), 221–228.
[24] G. Perelman, *The entropy formula for the Ricci flow and its geometric applications*, (2002): preprint arXiv:math/0211159.
[25] G. Perelman, *Ricci flow with surgery on three-manifolds*, (2003): preprint arXiv:math/0303109.
[26] G. Perelman, *Finite extinction time for the solutions to the Ricci flow on certain three-manifolds*, (2003): preprint arXiv:math/0307245.
[27] H. Terasaka: *On null-equivalent knots*, Osaka Math. J. **11** (1959), 95–113.
[28] V.G. Turaev: Quantum invariants of knots and 3-manifolds, de Gruyter Studies in Mathematics 18. Walter de Gruyter, Berlin, 1994.

Mathematical Institute, Tohoku University, Sendai, 980-8578, Japan
E-mail address: hironobu.naoe.p5@dc.tohoku.ac.jp